Journal of Power Sources 216 (2012) 15–21

Contents lists available at SciVerse ScienceDirect

Journal of Power Sources

journal homepage: www.elsevier.com/locate/jpowsour

Short communication

Proton exchange membrane micro fuel cells on 3D porous silicon gas diffusion layers

S. Kouassi [a], G. Gautier [a,*], J. Thery [b], S. Desplobain [a], M. Borella [c], L. Ventura [a], J.-Y. Laurent [b]

[a] GREMAN, UMR CNRS 7347, Université de Tours, 16 rue P. et M. Curie, 37071 Tours cedex 2, France
[b] LITEN, CEA Grenoble, 17 rue des Martyrs, 38054 Grenoble, France
[c] ALTATECH, 611 rue A. Berges, 38331 Montbonnot, France

HIGHLIGHTS

- We present a new approach to build miniaturized proton exchange membrane micro-fuel.
- We built fuel cells using 3D structured porous silicon substrates to increase the cell active surface.
- We performed fully porous "corrugated iron" like substrates by silicon electrochemistry.
- The prototype peak power performance was measured to be 90 mW cm^2 in a "breathing configuration" at room temperature.

ARTICLE INFO

Article history:
Received 20 March 2012
Received in revised form
2 May 2012
Accepted 16 May 2012
Available online 23 May 2012

Keywords:
3D
Porous silicon
PEMFC
Micro fuel cell

ABSTRACT

Since the 90's, porous silicon has been studied and implemented in many devices, especially in MEMS technology. In this article, we present a new approach to build miniaturized proton exchange membrane micro-fuel cells using porous silicon as a hydrogen diffusion layer. In particular, we propose an innovative process to build micro fuel cells from a "corrugated iron like" 3D structured porous silicon substrates. This structure is able to increase up to 40% the cell area keeping a constant footprint on the silicon wafer. We propose here a process route to perform electrochemically 3D porous gas diffusion layers and to deposit fuel cell active layers on such substrates. The prototype peak power performance was measured to be 90 mW cm^{-2} in a "breathing configuration" at room temperature. These performances are less than expected if we compare with a reference 2D micro fuel cell. Actually, the active layer deposition processes are not fully optimized but this prototype demonstrates the feasibility of these 3D devices.

1. Introduction

Miniaturization of fuel cells has been among the topic of great interest these last years due to the growing demand for high capacity batteries to supply more complex electronic devices. Many authors have underlined the potentiality of fuel cells to replace current leading edge technology based on lithium [1]. In fact, as a fuel cell can provide electrical energy as soon as it is fed with a fuel, the functioning time of the device is virtually unlimited. Nevertheless, many limitations have to be addressed to permit the hatching of this technology in the industry for mass market, such as the cost per watt.

When dealing with miniaturization of systems, MEMS (Micro-electro mechanical sytems) technology which follows from electronic devices microfabrication technology (with the additional mechanical features) has permitted many silicon based micro-systems production. In this field, porous silicon has already been used to perform with success MEMS devices like airbag igniters, gas sensors or pressure sensors [2]. For the latter reason, and considering porous silicon properties [3], this material has been therefore a natural candidate for miniaturization of fuel cells when starting from a silicon substrate. Then, porous silicon can be integrated in fuel cells in different manner. In fact, it can be integrated as hydrogen source in the gas feed system or in the core system. There it can act as the membrane support of the fuel cell [4]. But it can be also the mechanical support acting as a flowfield, gas diffusion layer and/or catalyst support of the cells (see [5,6 or 7] for example).

We propose in this article an original approach which opens a route to the miniaturization of fuel cell through a 3D approach. We will present in this article the process for the realization of the 3D silicon support and the deposition of the fuel cell active layer. The porous substrates were characterized via permeation

* Corresponding author. Tel.: +33 0 47 42 40 00; fax: +33 2 47 51 01 34.
E-mail address: gael.gautier@univ-tours.fr (G. Gautier).

0378-7753/$ – see front matter © 2012 Elsevier B.V. All rights reserved.
doi:10.1016/j.jpowsour.2012.05.046

measurements and the fuel cell performances were measured. The results are discussed and compared with the one obtained for a planar substrate.

2. Experimental

2.1. Fabrication of 3D single side porous silicon substrates

We used (100) n-type silicon wafers with a doping concentration of 10^{14} at.cm^3 (26–33 Ω cm). These 6 inches wafers are 560 μm thick and polished on both sides. We performed 3D structures on these wafers using anisotropic wet etching. To produce 3D shapes, we performed the process presented in a cross section schematic view on Fig. 1. As a first step, a photolithography is performed on both side of the silicon wafer on which a 2.3 μm thermal oxide has been grown (Fig. 1a). The fuel cell active regions where the 3D structures will be performed are opened using a BOE (Buffered Oxide Etch) solution (Fig. 1b). Then, a thin 300 nm thick thermal oxide layer is produced in the opened areas (Fig. 1c). Afterward, a second photolithography step is performed to carry out rectangular patterns through this thin oxide. To produce the 3D structures (Fig. 1d), the wafer is etched at 85 °C in a TMAH (Tetra-methyl–ammonium hydroxide) solution having a concentration of 18% wt. This anisotropic etching produces walls with an angle of 54.7° [8], this enables us to develop the surface of the GDL to a factor of 1.4 when the trenches have a complete V shape.

Removal of the thin residual oxide layer is carried out using a BOE treatment. This led us to a textured area free of oxide and a surrounding area still protected with an oxide layer of about 2 μm. An *in situ* n^+ doped polycrystalline silicon layer is then deposited on both sides of the substrate by LPCVD (Low Pressure Chemical Vapor Deposition) using silane and phosphine gases (Fig. 1e). This layer enables the ohmic contact on the backside during electrochemical etching, it also permits the protection of the insulating oxide layer against HF [9]. After this step, the 6 inches wafer presents 34 textured areas of 1 cm^2 ready to be anodized in a HF based electrolyte.

After the 3D microfabrication process, the silicon wafers were electrochemically etched in a double tank electrochemical cell developed by AMMT. The wafer is placed between two 6 inches meshed platinum electrodes. The anodization side is considered as the front side of the substrate. The backside is illuminated during the anodization process using a 150 W halogen lamp. This is mandatory to provide holes in low doped silicon bulk. To produce

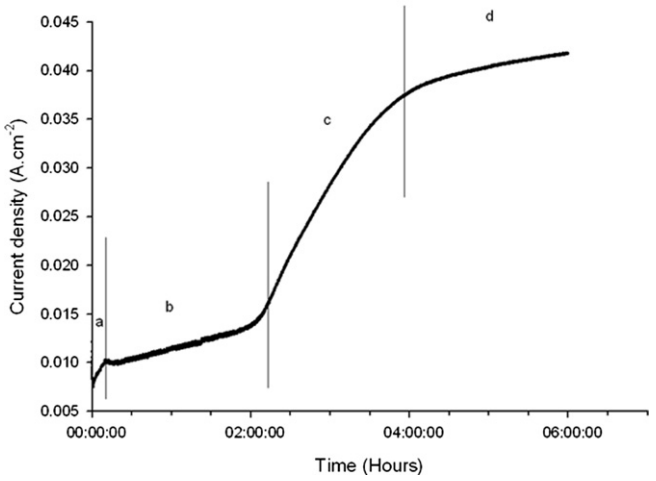

Fig. 2. Current density evolution during an anodization at 3.1 V (potentiostatic etching). The curve can be separated in 4 distinct steps: (a) pore initiation, (b) macropore growth through the substrate, (c) first macropores going through the substrate, (d) end of the reaction.

macropores going through the entire silicon substrate thickness, we have achieved a potentiostatic anodization at 3.1 V in a HF:CH_3COOH:H_2O (3.2:1.5:1) electrolyte. A typical current density evolution during macropore formation in potentiostatic conditions on the patterned 6 inches substrates (34 areas of 1 cm^2) is presented on Fig. 2. The first step (Fig. 2a) is correlated to the pores initiation process on the silicon substrate surface [10]. Then, the etching current during pores growth in the substrate rises slowly (Fig. 2b). After this step, a great increase of the current due to the first pores coming through the opposite face of the substrate is observed.

These pores produce a path for the electrolyte between the 2 cells constitutive of the electrochemical set-up. This path lowers the global resistance of the system. To overcome this effect, the current increases according to the number of pores going through the wafer (Fig. 2c). This current increase maintains a high etching rate during pores formation. Finally, when a majority of pores have run through the substrate, the current becomes almost constant (Fig. 2d). The resulting pores were 3–5 μm in diameter. Moreover, the macropores etched in this high resistivity n type material (26–33 Ω cm) and moderate current densities are current line driven [11]. As a consequence, the pores are meandrous. Moreover,

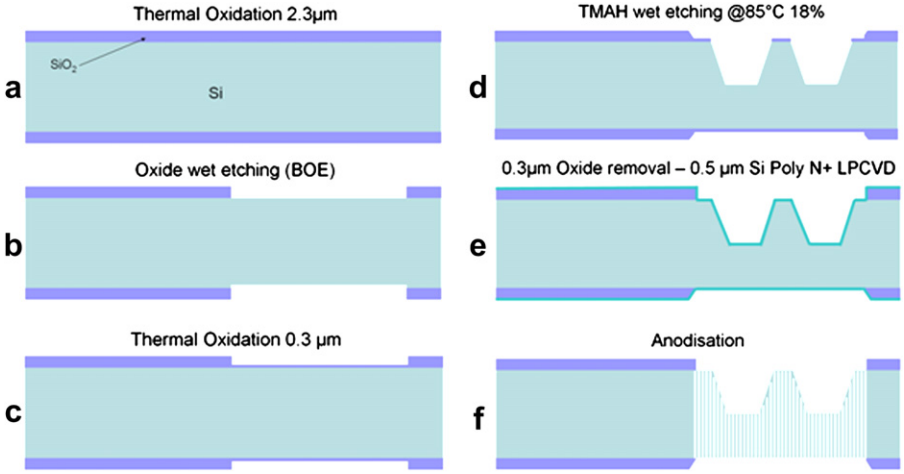

Fig. 1. Cross section schematic view of the process steps performed to obtain single side 3D porous substrates on 6 inches silicon wafers.

the macropores which went through the substrate show a widening of their section from the beginning to the end of the process leading to larger pores opening at the emerging side of the substrate (about 10 μm).

After the electrochemical etching, a slight RIE etching has to be carried out on the wafer backside in order to open all macropores. Wet etching techniques can also be performed through a low concentration KOH etching to carry out opening of all macropores as demonstrated in previous work [12]. The resulting structure is presented in the Fig. 3.

The reaction occurring at the anode can be summarized with equation (1) [13].

$$Si + h^+ + 4HF_2^- \rightarrow SiF_6^{2-} + 2HF + H2 + e^- \quad (1)$$

This equation points out the necessity of holes to perform porous silicon etching. In some parts of the substrates, there is a lack of holes due to the varying thickness of the 3D topographies. Indeed, for highly resistive n-type materials, the electrochemical etching is dominated by holes diffusion in the entire bulk [14]. As a consequence, only a reduced fraction of the backside surface can be opened.

Otherwise, the carriers tend to accumulate mainly at the edges between two surfaces when they present an angle lower than 180°. As a consequence, we observe over-etching in those regions.

2.2. Fabrication of the "corrugated-iron" like porous structures

In the case of highly doped silicon, the electrochemical reaction is locally activated by tunneling of holes [15]. This mechanism is homogeneous at the silicon–electrolyte interface and produces a thin mesoporous silicon layer. Thereby, a doping of the surface was added to the micro-fabrication process. This step is performed before the LPCVD deposition of the polycrystalline doped layer. It consists in a $POCl_3$ pre-deposition treatment and subsequently a thermal treatment of 240 min at 1150 °C.

To get around the non homogeneous etching through the substrate (see the previous part), we modified the process in order to grow pores on the whole surface. To do so, we modified the architecture for a 3D structure with a homogeneous thickness profile. This modification was carried out to increase the amount of pores going through the substrate. This new step consists in an anisotropic wet etching on both sides of the wafer to perform

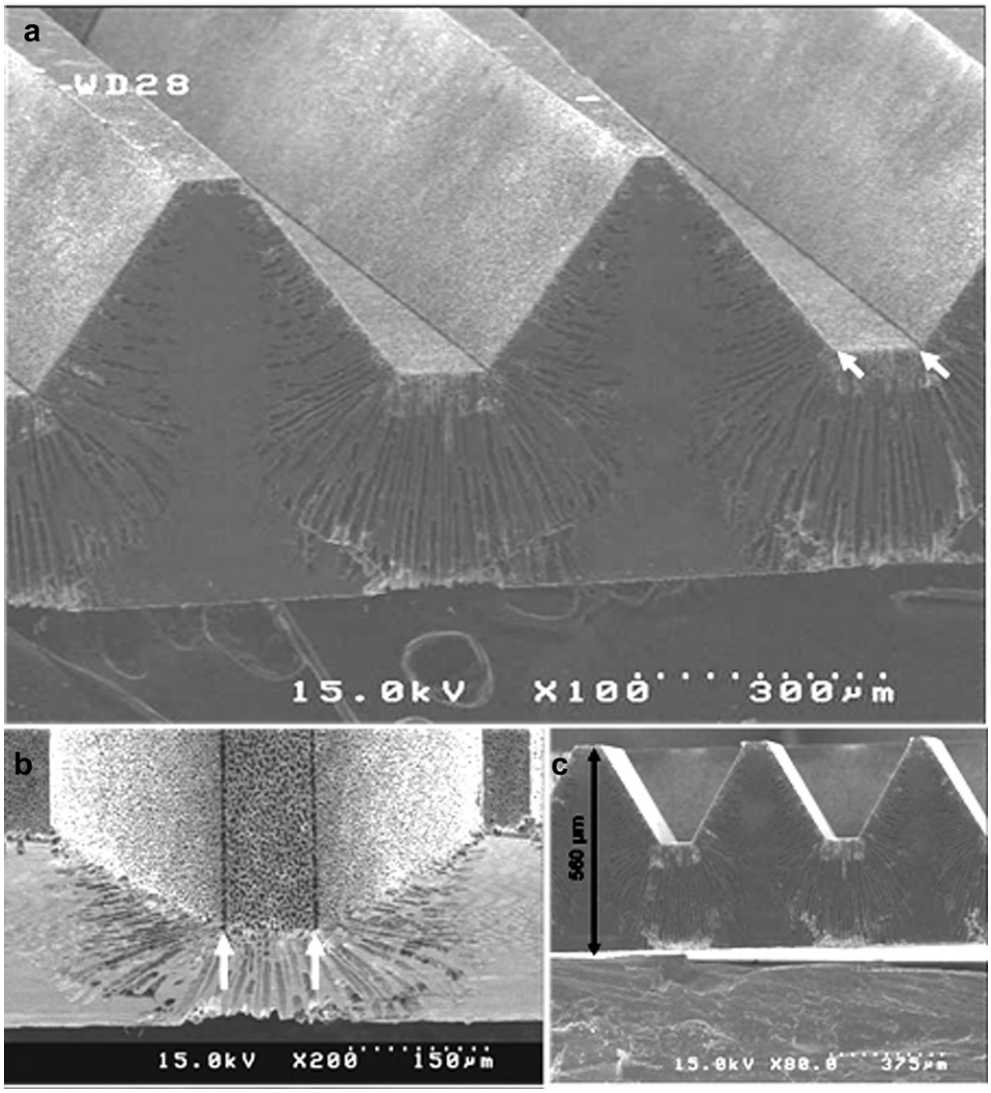

Fig. 3. 3D single side 560 μm thick substrate SEM images after porous silicon formation. An electrochemical etching at 3.1 V potential during 270 min has been performed. The arrows indicate the trails due to over etching.

a "corrugated iron" like structure. The results obtained after the electrochemical etching of this modified structure (doping layer and TMAH etching on both faces) are presented on Fig. 4. These structures performed have been etched in a HF mixture in potentiostatic conditions (@3.1 V). In this case, all the macropores initiated on the top face went through the substrate, except for a very small zone (between the 2 dotted lines in Fig. 5b). This might be due to a lack of holes generation on the backside in this region.

2.3. Deposition of the fuel cell active layers

The 1 cm^2 fuel cells were directly manufactured on the porous silicon substrate with thin film deposition techniques. The various layers of these micro fuel cells are presented schematically on Fig. 5. The 500 nm thick gold collectors were deposited with cathodic sputtering and the catalytic layers were deposited with spraying a C/Pt ink [16]. The proton exchange membrane was performed spraying a commercial Nafion® 1021 solution. Conventional spraying and jetting techniques did not allowed depositing homogeneous Nafion® membranes on 3D structures and consequently a specific atomized spray nozzle was used. These techniques allowed us to perform quasi-conformal layers on the corrugated silicon surface. Nevertheless, it has to be pointed out that the AR (Aspect Ratio) has a great influence on the conformity of the different layers deposited using these techniques (sputtering and spray coating). Therefore, the process identified for one AR is not valuable for a large range of AR. The spray coating parameters were defined through a set of experiments to adjust the process parameters. Then, the spray coating used to perform the active layers of the final tested fuel cell was realized with an ink pressure of 0 bar, a spray pressure of 0.5 bars, at a temperature of 70 °C and a distance substrate/print head of 20 mm. The conformal layers were produced through a multiple deposition process on the heated substrate.

The previously described macroporous silicon substrates have been integrated as support of the fuel cell active layers. The Fig. 6 presents a cross section of the stack after deposition of the successive layers and it shows a quite uniform coverage on the 3D silicon structure. To clearly identify the distinctive layers, some complementary observations have been performed using FIB (Focused Ion beam) (See Fig. 7). The morphology of the Nafion® 10–21 membrane is stringy because of the degradation of the polymeric material by the ion beam. Nevertheless, we can clearly see in the Fig. 7 that the layers are in close contact and well stacked. From thicknesses measurements, we can assume that the catalyst layer thickness varies between 2 and 5 μm and the Nafion® thickness varies between 25 and 45 μm.

2.4. Characterization methods

The polarization curves were measured with a VMP3 (biologic and Co.) potentiostat in galvanostatic cyclic mode. Before each

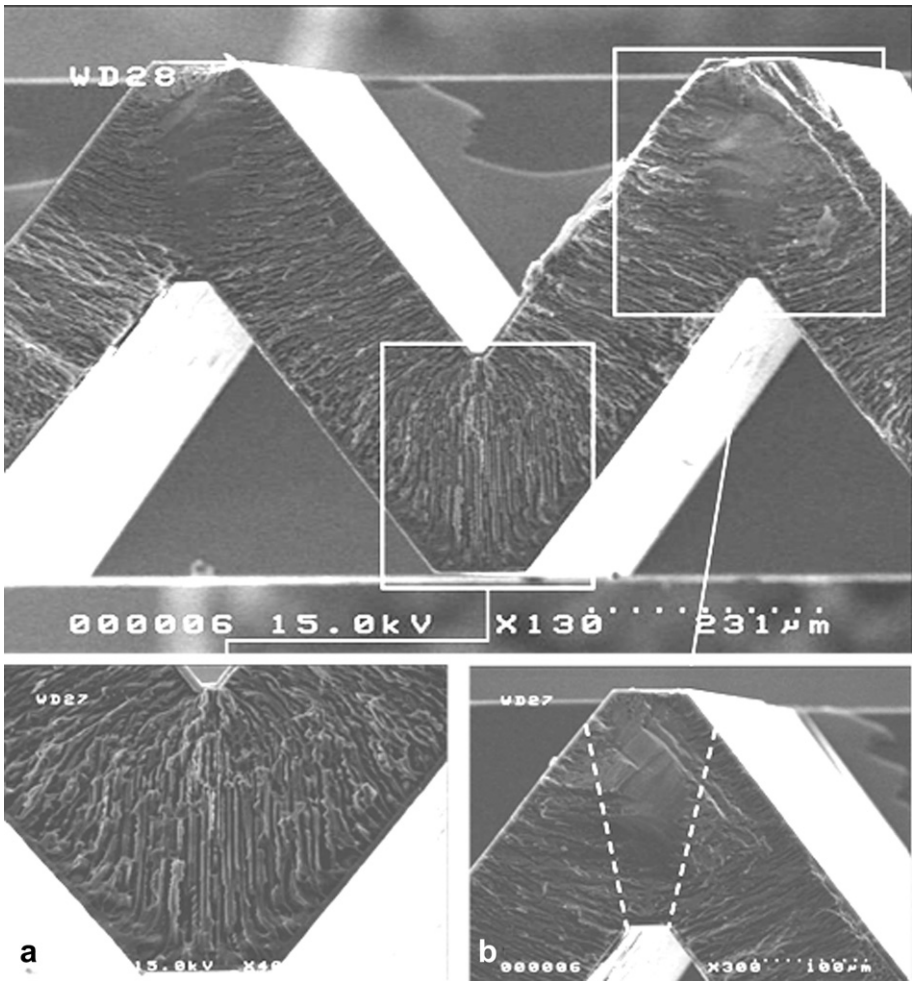

Fig. 4. "Corrugated iron like" structures after an electrochemical etching at 3.1 V for 240 min. The dotted lines on Fig. 4b indicate the region where no pore growth occurred. Note that the anodized surface is on top and the illuminated backside is at the bottom on those pictures.

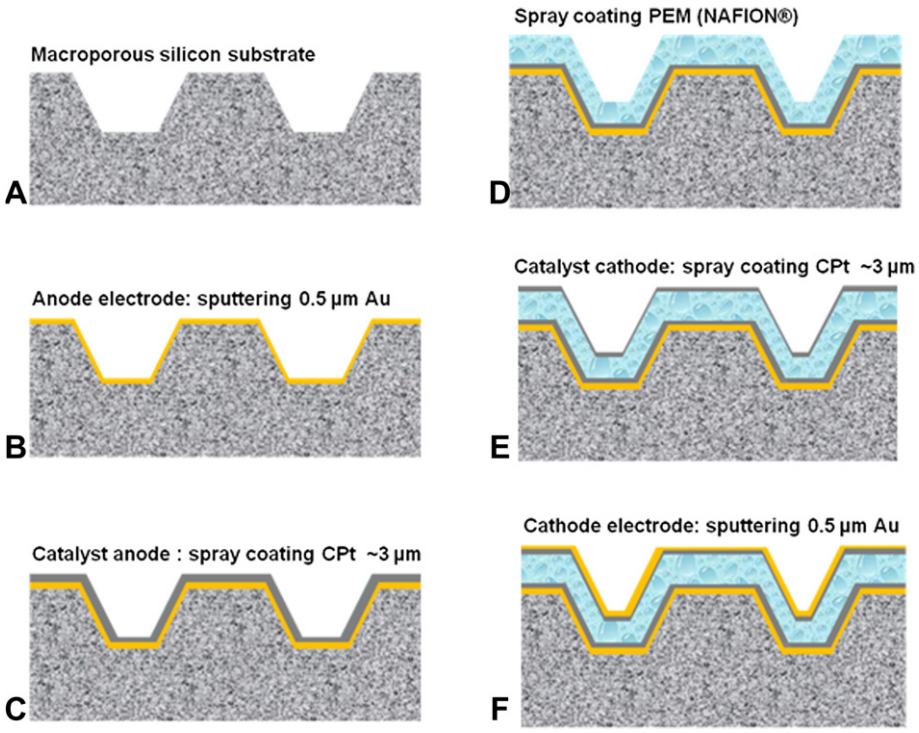

Fig. 5. Cross section schematic view of the process steps performed for the fuel cell active layers deposition. The anode and cathode collectors are performed using sputtering deposition. The other layers (catalyst and membrane) are deposited using spray coating.

measurement, the OCV (Open Circuit Voltage) was stabilized 10 min. The tests were performed at room temperature, in ambient conditions. The substrate porosity has been evaluated through permeability measurements. To perform this measurement, different H_2 gas pressures are applied on one side of the porous silicon membrane and the flow rate is measured after the membrane. The set up used to perform these measurements is built up with a hydrogen supplier, a regulator, a manometer for measurement, a water column, a sample holder and 2 flow meters. The gas is provided on demand using the regulator and the water column to set the pressure arriving on the backside of the porous sample. The porous sample is placed in the holder and sealed with toric rings. The pressure is measured before the sample with the manometer. The flow is measured before the sample and after the sample using the 2 flow meters.

Using this system, we are able to set and monitor the upstream pressure and measure the incoming flow as well as the flow coming out of the membrane. The flow is measured for different pressure and divided by the opened surface to obtain the flow per unit area.

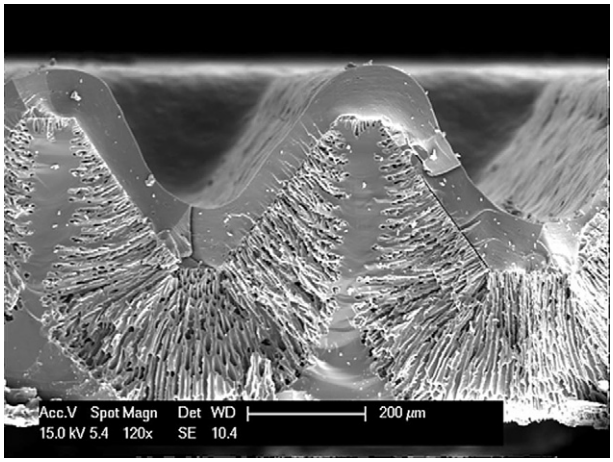

Fig. 6. Structured porous silicon substrate after successive deposition 150 layers of Nafion ink using spray coating leading to a thickness $e = 80$ µm.

3. Results and discussion

3.1. Hydrogen flow rate measurements

The hydrogen flow rates were measured for the different 3D structures performed (single side and double side structured substrates) and the results are plotted on Fig. 8. The flow rates measured for the corrugated iron like substrates are about 3 times superior to the values on single side structured substrates. This is consistent with the observation of an enhanced density of crossing macropores for these last. As 4 ccm flow rate theoretically leads to 500 mW cm^{-2} of maximum power density, the measured flow rates are largely sufficient for the considered application.

3.2. Electrical performances and discussion

Electrical tests have been performed to evaluate the performances of the fuel cells. Two probes are used to perform a wafer level reliability test of the cells (see Fig. 9). One probe is connected with the anode and the other with the cathode of a fuel cell unit. The wafer is placed in such a way that the holder presenting a cavity is sealed with the wafer on top. Then, hydrogen arrives on the bottom of the wafer through this cavity. The upper side is exposed to air (air breathing tests). A typical polarization curve of an operating 3D fuel cell is presented on Fig. 10. The measured OCV (Open Circuit Voltage) is about 0.9 V and the power peak value is around 90 mW cm^{-2} at 0.4 V. Previous work performed by our

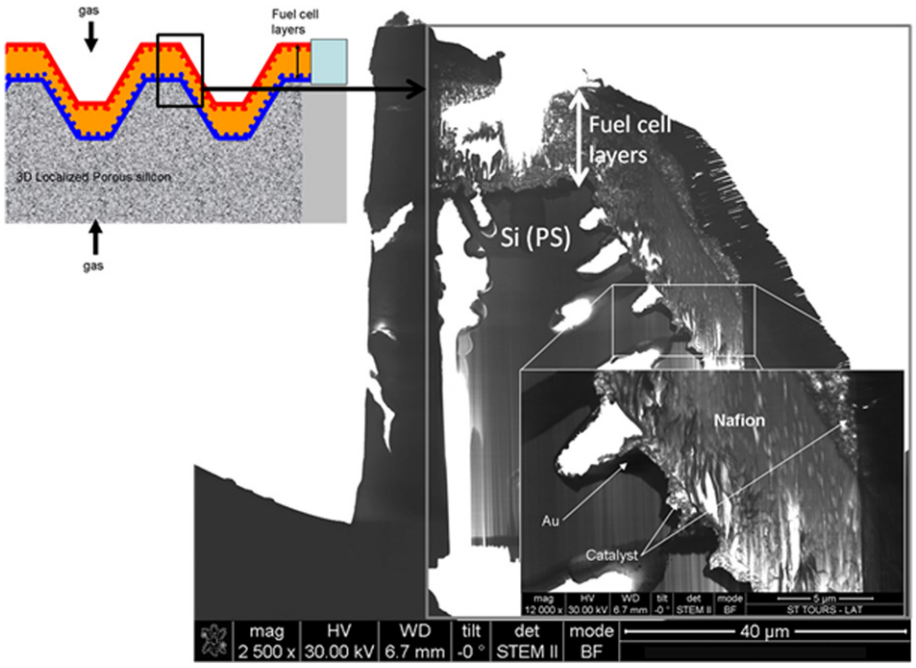

Fig. 7. FIB cross section (right handside) of the stack performed on top of a macroporous trench (PS) as illustrated with the schematic view of the fuel cell stack (top left handside). The different layers can be identified by density difference. The polymer membrane (nafion) has been partially removed due to the ion beam.

group on planar macroporous silicon stacks led to 250 mW cm^{-2} [17]. If we consider the 3D substrate active area expansion, the results obtained here are therefore under the expected value (around 350 mW cm^{-2}). Some parameters may be considered to explain these results. Compared with the performance we had on a 2D porous silicon, the overall thickness of the Nafion® layer is multiply by 2 and the homogeneity on 3D surfaces needs thus to be optimized. Moreover, the Nafion© is deposited by spray coating and the final quality of the membrane could be quite different from planar structures. Secondly, the complex 3D structure can lead to an increase of the collector resistances or a lowering of the catalyst efficiency.

Finally, the macroporous substrates used to perform this first test are single-side etched wafers with a small area of permeation; we expect a good improvement of the future stacks using corrugated iron like structures. Currently, the same experiments are performed on those substrates to compare the effect of this improved structure on the cell performance.

In addition, we can notice that most of the micro fuel cell processes reported in the litterature involve standard technologies such as DRIE or KOH wet etching [18,19]. The use of microporous or mesoporous silicon as a gaz diffusion layer is also investigated but the size of the pores limits the performances. For instance, D'arrigo et al. reports a maximum power density of 62 mW cm^{-2} under pure H_2 and O_2 (80 sccm) [5]. Macroporous seems to be more valuable to perform high performances as the pores are larger in diameter. Lee and coworkers reported power densities around 170 mW cm^{-2} on macroporous planar substrates with an OCP of 0.9 V. These

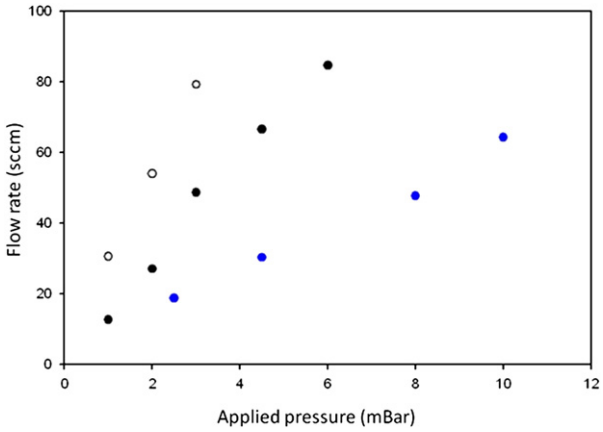

Fig. 8. Flow rate per square centimeter measured regarding the applied pressure on various 3D structures. The blue circles correspond to a single side 3D porous substrate. Greatly improved flow rates were measured on corrugated iron like structures after a backside RIE process (black circles) and a HF-KOH-HF wet etching process (open circles).

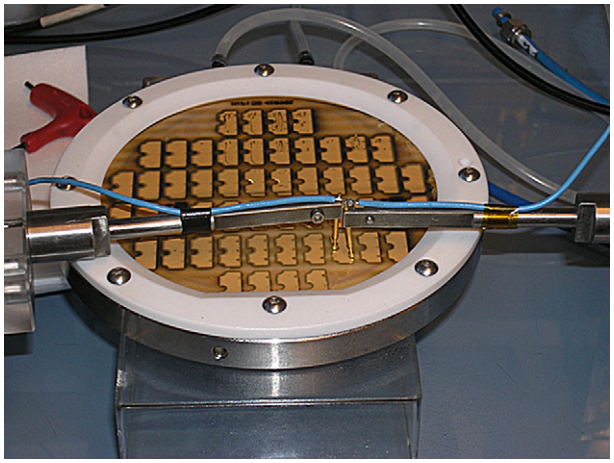

Fig. 9. Photography of the wafer level reliability test set-up used to perform operation measurements of the miniaturized fuel cell. The wafer backside is sealing a cavity fed with hydrogen allowing this gas to be provided at the anode (bottom of the stack). Air breathing is provided on the top of the fuel cells.

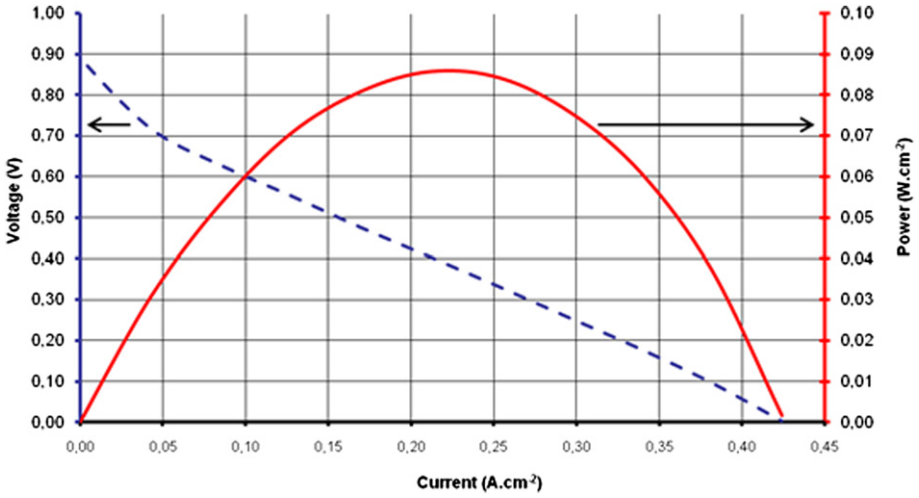

Fig. 10. Measurements of the voltage (left scale bar) and the power density value (right scale bar) as a function of the current for a 1 cm^2 surface at room temperature with a sweep rate of 10 mVs^{-1}.

performances are comparable with our work even if they are not obtained in a breathing configuration but under pure oxygen [20].

4. Conclusions

Breathing fuel cells were realized on porous silicon substrates using printing techniques. The silicon substrate was found suitable to supply high gas flow rates and maintain cohesion of the various layers that are deposited in a liquid form. With the will to increase the performance of the planar fuel cells, 3D porous silicon substrates were realized. Two 3D structures were developed, a one side structured and a double side structured substrates. It was shown that double side structures favor a homogeneous opening of the macropores. The process for the realization of fuel cells on 3D shapes was adapted via the addition of a Nafion® 10–21 spraying step for the deposition of a conformal electrolytic layer. A respective power density of 250 mW cm^{-2} and 90 mW cm^{-2} were measured for the 2D and 3D structure. An optimization of the process on 3D structures is still required for an enhancement of the performances.

Acknowledgements

This work has been supported by the French National Research Agency (ANR) through the programm PanH 2006 with the MICONOS project.

References

[1] C.K. Dyer, Journal of Power Sources 106 (2002) 31–34.
[2] V. Lindroos, M. Tilli, A. Lehto, T. Motooka, Handbook of Silicon Based MEMS Materials and Technologies, William Andrew Pub., 2010.
[3] S. Desplobain, G. Gautier, N. Gharbage, L. Ventura, M. Roy, Physica Status Solidi (c) 5 (2008) 3843–3845.
[4] T. Pichonat, B. Gauthier-Manuel, Journal of Micromechanics and Microengineering 15 (2005) S179–S184.
[5] G. D'arrigo, C. Spinella, G. Arena, S. Lorenti, Materials Science and Engineering: C 23 (2003) 3–18.
[6] Y. Yamazaki, Electrochemica Acta 50 (2004) 663–666.
[7] M. Hayase, T. Kawase, T. Hatsuzawa, Electrochemical and Solid-State Letters 7 (2004) A231–A234.
[8] J.T.L. Thong, W.K. Choi, C.W. Chong, Sensors and Actuators A 63 (1997) 243–249.
[9] G. Kaltsas, A. Nassiopoulos, Sensors and Actuators A 65 (1998) 175–179.
[10] M.H.A. Rifai, M. Christophersen, S. Ottow, J. Carstensen, H. Foll, Journal of the Electrochemical Society 147 (2000) 627–635.
[11] V. Lehmann, Thin Solid Films 255 (1995) 1–4.
[12] S. Kouassi, G. Gautier, S. Desplobain, L. Coudron, L. Ventura, Defect and Diffusion Forum 297-301 (2010) 887–892.
[13] V. Lehmann, Electrochemistry of Silicon, Wiley-VCH Weinheim, 2002.
[14] P. Steiner, W. Lang, Thin Solid Films 255 (1995) 52–58.
[15] V. Lehmann, R. Stengl, A. Luigart, Materials Science and Engineering 69 (2000) 11–22.
[16] J. Thery, S. Martin, V. Faucheux, L. Le Van Jodin, D. Truffier-Boutry, A. Martinent, J.-Y. Laurent, Journal of Power Sources 195 (2010) 5573–5580.
[17] S. Desplobain, G. Gautier, P. Bouillon, L. Ventura, Physica Status Solidi (a) 206 (2009) 1282–1285.
[18] L. Zhu, K. Lin, R.D. Morgan, V.V. Swaminathan, H.S. Kim, B. Gurau, D. Kim, B. Bae, M.A. Shannon, Journal of Power Sources 185 (2008) 1305–1310.
[19] J. Yeom, R.S. Jayashree, C. Rastogi, M.A. Shannon, P.J. Kenis, Journal of Power Sources 160 (2006) 1058–1064.
[20] S.J. Lee, Y.M. Lee, C.Y. Lee, J.J. Lai, F.H. Kuan, C.W. Chuang, Journal of Power Sources 171 (2007) 148–154.